Supporting Information

Materials: All starting materials were purchased from commercial suppliers and used without further purification unless otherwise noted.

Measurements: FT-IR spectra were obtained on the Nicolet IS50 Fourier transform infrared spectrometer. ^{13}C CP/MAS solid-state NMR spectra were performed on a Bruker Avance III model 400 MHz NMR spectrometer at a MAS rate of 5 kHz. X-ray diffraction (XRD) measurements were carried out using the DMax 2200PC X-ray diffractometer. The surface area and pore size distribution were obtained with the Micromeritics ASAP 2020M Accelerated Surface Area and Porosimetry System. Scanning electron microscopy (SEM) was performed with a Hitachi SU8010 field-emission scanning electron microscope. Ion concentrations were determined using an inductively coupled plasma atomic emission spectrometer (ICP-AES). X-ray photoelectron spectroscopy (XPS) measurements were conducted on an Escalab-MK II photoelectronic spectrometer with Al Kα (1200 eV). Elemental analysis (for C, H, O, N) was measured using a Perkin Elmer 2400 Series II CHNS/O Analyzer.The pH of the solution was measured using the PHS-3C pH meter.

Preparation of CMP-DVB-AO. Briefly, 1 mmol p-divinylbenzene, 1 mmol 4-cyanostyrene and 1% weight AIBN were stirred under a nitrogen atmosphere at 60 °C for 24h. Subsequently, the mixture was filtered, and the product was washed with 1 M HCl, methanol, acetone, chloroform and dried under vacuum at 60 °C to obtain a white CMP-DVB solid. Then, 100 mg of CMP-DVB, 500 mg of triethylamine and 750 mg of hydroxylamine hydrochloride were suspended in 20 mL ethanol, and the reaction mixture was stirred at 70 °C for 48 h. Subsequently, the mixture was filtered, and the product was washed with methanol and dried under vacuum at 40 °C to obtain an orange solid of CMP-DVB-AO.

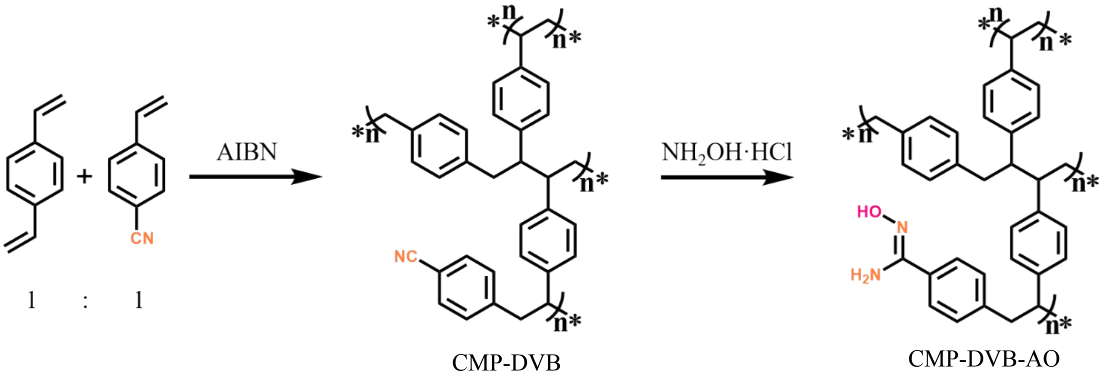

Figure S1 Schematic illustration of CMP-DVB-AO: (a) AIBN, 60 °C, 24 h. (b) $NH_2OH \cdot HCl/N(CH_2CH_3)_3/EtOH$, 70 °C, 48 h.

Preparation of PAF-170-AOs series. Aluminium chloride (500 mg) was suspended in 40 mL chloroform, and this mixture was stirred under a nitrogen atmosphere at 60 °C for 3 h. Then, a solution consisting of biphenyl and cyanobenzene (ratios: 4:1; 2:1; 1:1; 1:2; 1:4) and suspended in 20 mL chloroform was injected into it. The reaction system was stirred at 60 °C for 48 h. Subsequently, it was filtered, and the product was washed with 1 M HCl, methanol, acetone, chloroform and dried under vacuum at 60 °C to obtain brown solid PAF-170 series. Then 100 mg of PAF-170 series, 500 mg of triethylamine and 750 mg of hydroxylamine hydrochloride were suspended in 20 mL ethanol, and the reaction mixture was stirred at 70 °C for 48 h. After filtered, the product was washed with methanol and dried under vacuum at 40 °C to obtain brown solid PAF-170-AO series.

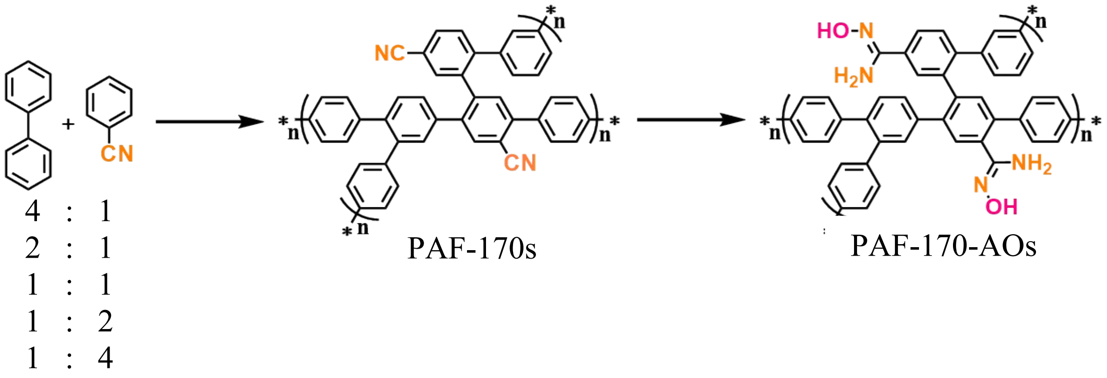

Figure S2 Schematic illustration of PAF-170-AOs: (a) $AlCl_3/CHCl_3$, 60 °C, 48 h. (b) $NH_2OH{\cdot}HCl/N(CH_2CH_3)_3/EtOH$, 70 °C, 48 h.

Preparation of PAF-170 (171, 172)-AO. Aluminium chloride (500 mg) was suspended in 40 mL chloroform, and this mixture was stirred under a nitrogen atmosphere at 60 °C for 3 h. Then, the solution of 1 mmol of biphenyl (*p*-terphenyl and 1,3,5-triphenylbenzene) and 2 mmol cyanobenzene suspended in 20 mL chloroform was injected into it. The reaction system was stirred at 60 °C for 48 h. Subsequently, it was filtered, and the product was washed with 1 M HCl, methanol, acetone, chloroform and dried under vacuum at 60 °C to obtain brown solid PAF-170(171, 172). Then, 100 mg of PAF-170(171, 172), 500 mg of triethylamine and 750 mg of hydroxylamine hydrochloride were suspended in 20 mL ethanol, and the reaction mixture was stirred at 70 °C for 48 h. After filtered, the product was washed with methanol and dried under vacuum at 40 °C to obtain brown solid PAF-170(171, 172)-AO.

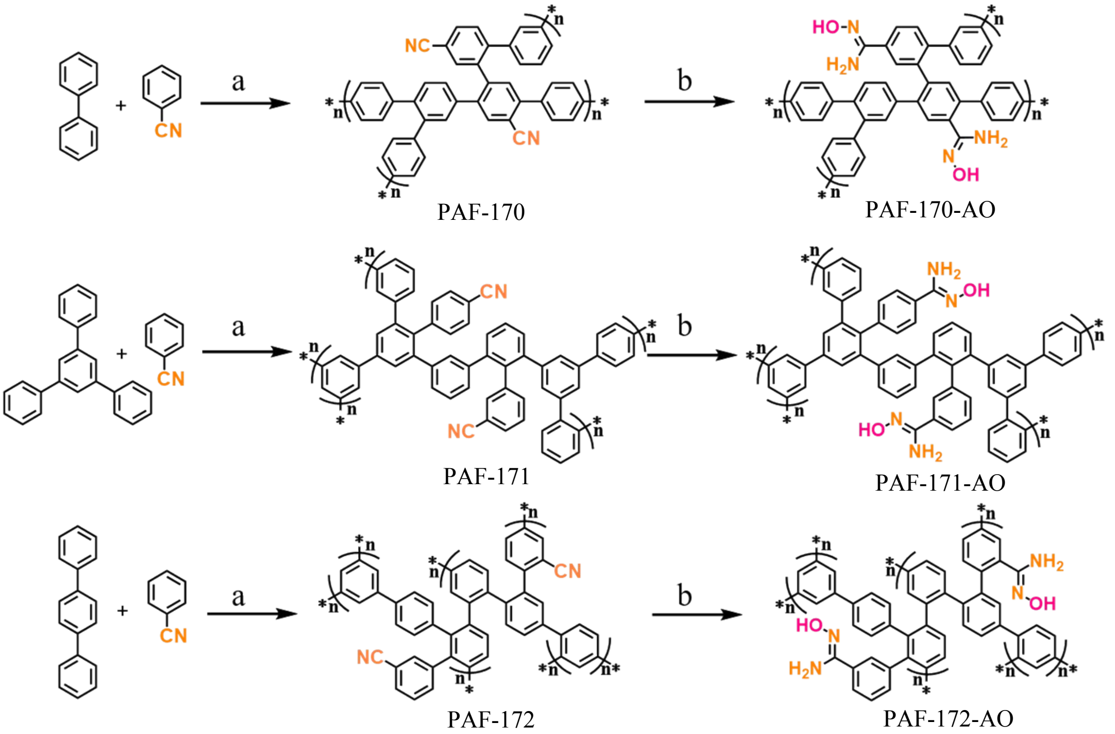

Figure S3 Schematic illustration of PAF-170/171/172-AO: (a) $AlCl_3/CHCl_3$, 60 °C, 48 h. (b) $NH_2OH \cdot HCl/N(CH_2CH_3)_3/EtOH$, 70 °C, 48 h.

Sorption experiments

The aqueous solutions with different uranium concentrations were obtained by diluting the stock $UO_2(NO_3)_2 \cdot 6H_2O$ solution with the proper amount of distilled water unless otherwise indicated. The pH levels of the solutions were adjusted by HNO_3 or NaOH aqueous solution. The concentrations of uranium during all the experiments were detected by inductively coupled plasma-optical emission spectroscopy (ICP-OES) and inductively coupled plasma-mass spectrometry (ICP-MS) for extra low concentrations. All the adsorption experiments were performed at ambient conditions.

Uranium adsorption capacity tests. To get uranium sorption isotherms for PAF adsorbents, PAF adsorbents were suspended in U(VI) solution from 1 to 85 ppm at pH 6 and stirred at a constant rate at room temperature for 24 h. The treated solutions were filtrated through a 0.45 μm membrane filter. The supernatant was analyzed using ICP analysis to determine the remaining uranium concentration. The uptake of uranium ion was determined by the equation:

$$Q_e = \frac{c_o - c_e}{m} \times V$$

Q_e (mg g^{-1}) represents the uranium uptake, C_0 and C_e are the initial and equilibrium concentrations, V is the volume of solution, and m is the weight of PAF material.

Uranium sorption kinetics tests. To test the uranium sorption kinetics for PAF adsorbents, PAF adsorbents was suspended in 2 L 7 ppm U(VI) solution at pH 6 and also stirred at a constant rate at room temperature. At appropriate time intervals, 5 mL solution was taken from the mixture, and the solutions were filtrated through a 0.45 μm membrane filter. The supernatant was analyzed using ICP analysis to determine the uranium concentration.

The adsorption capacity calculated by the equation:

$$Q_T = \frac{c_0 - c_e}{m} \times V$$

Where, Q_T (mg g^{-1}) is the uranium ion uptake, C_0 and C_e are the initial and equilibrium concentrations, V is the volume of solution, and m is the weight of PAFs material

Uranium adsorption capacity and sorption kinetics calculation.

The uranium adsorption capacity was calculated by using these models:

The Langmuir model is expressed by the equation:

$$\frac{C_e}{q_e} = \frac{1}{q_{max} \times k_L} + \frac{C_e}{q_{max}}$$

where C_e is the equilibrium concentration (mg·L^{-1}), q_e is the equilibrium adsorption capacity (mg·g^{-1}), q_m is the maximum adsorption amount at the time of equilibrium (mg·g^{-1}), and k_L is the Langmuir adsorption constant (L·mg^{-1}).

The Freundlich model is expressed by the equation:

$$\ln q_e = \ln k_F + \frac{1}{\mathrm{n}} \ln C_e$$

where C_e and q_e are the equilibrium concentration and adsorption capacity, respectively, k_F is the Freundlich isotherm constant, and n is the Freundlich exponent.

The two adsorption models mentioned above can be described mathematically as follows:

$$\log(q_e - q_t) = \log q_e - \frac{k_1}{2.303} \times t$$

$$\frac{t}{q_t} = \frac{1}{k_2 \mathrm{q_e}^2} + \frac{1}{\mathrm{q_e}}$$

where q_t (mg·g^{-1}) and q_e (mg·g^{-1}) are the amounts of adsorbed metal ions at a certain time t (min) and at equilibrium time, respectively; k_1 (min^{-1}) and k_2 (g·mg^{-1}·min^{-1}) are the pseudo-first-order adsorption, and pseudo-second-order adsorption constants, respectively.

Selectivity tests. To a 1 L solution of various metal ions (V^{5+}, Zn^{2+}, K^+, Ca^{2+}, Na^+, Mg^{2+}, Pb^{2+}, Ni^{3+}, Fe^{3+}, Cu^{2+}, Co^{2+}, Li^+, Mn^{2+}, Cr^{3+} and Cd^{2+}) at the same concentration (5 ppm) associated with uranyl (5 ppm) competition in natural seawater in an Erlenmeyer flask with a magnetic stir bar, 5 mg PAF adsorbent was added. After being stirred at room temperature for 24 h, 5 mL solution was taken from the mixture, and the adsorbent was separated by syringe filter (0.45 μm membrane filter). The uranium concentration in the resulting solutions was analyzed by ICP-MS. And the distribution coefficient (K_d) is the partition coefficient used to compare the affinity of the adsorbent for a certain ion, i.e., to evaluate the uptake ability of the adsorbent to the ions. The K_d values of PAF-170-AO was thus calculated with 5 ppm uranium in simulated seawater solution (10 mL) in the presence of adsorbents (5 mg). The affinity of PAF-170-AO for uranium was verified by calculating K_d.

$$K_d = \frac{(C_i - C_e)}{C_e} \times \frac{V}{m}$$

where C_i ($mg \cdot L^{-1}$) and C_e ($mg \cdot L^{-1}$) are the initial and equilibrium concentrations of the metal ion, respectively, $V$is the solution volume (mL), and m is the mass of the adsorbent (mg).

Reusability tests. To test the reusability of the adsorbents, the uranium on adsorbent was eluted with the elution solution of 1 M Na_2CO_3 and reused for uranium adsorption capacity assay.

Uranium recovery from natural seawater. To determine the uranium adsorption capacity of the adsorbent in natural seawater, the 5 mg PAF adsorbent was-loaded on porous ceramic sheet (the sheet has diameter of 2.5 cm and thickness of 3 mm) was used. The flow rate was controlled 5 L/min by motor controller. The field test was lasted for 9 weeks. A 100 L of natural seawater in total was used for the entire experiment at room temperature. The adsorption capacity of the adsorbent to metal ion were determined by detected the concentration of the metal ion before and after the adsorption process by using inductively coupled plasma mass spectrometry ICP-MS.

Results and Discussion

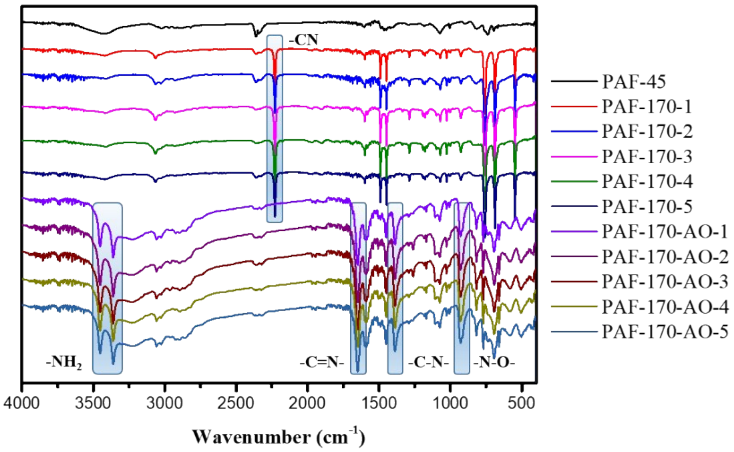

Figure S4 Fourier transform infrared (FT-IR) spectra for PAF-45, PAF-170s and PAF-170-AOs. Scanning range is 400-4000 cm^{-1}.

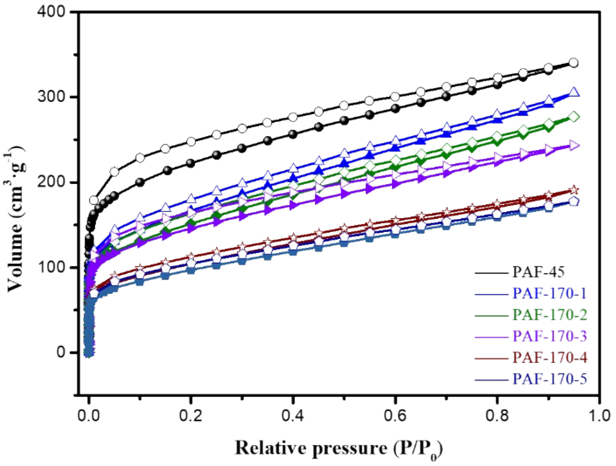

Figure S5 N_2 adsorption isotherms (solid icons) and N_2 desorption isotherms (hollow icons) collected at 77 K of PAF-45 and PAF-170s.

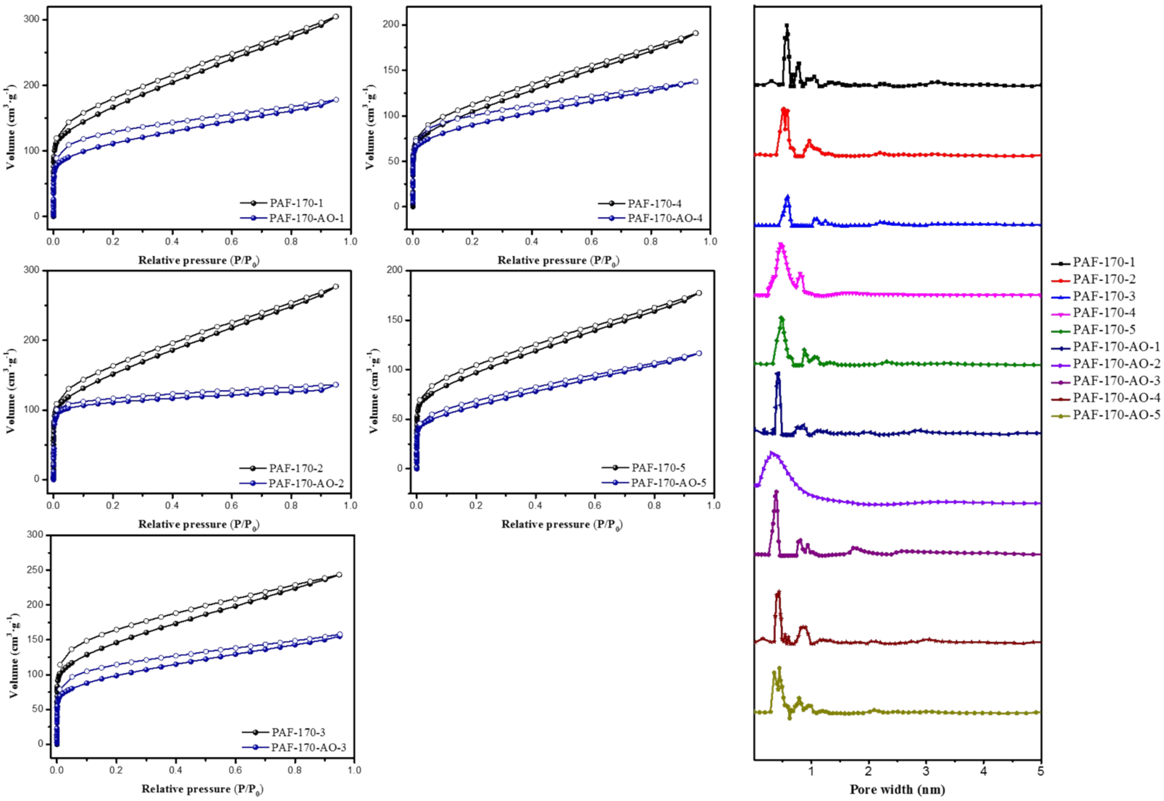

Figure S6 N_2 adsorption isotherms (solid icons) and N_2 desorption isotherms (hollow icons) and distribution of pore size collected at 77 K of PAF-170s and PAF-170-AOs.

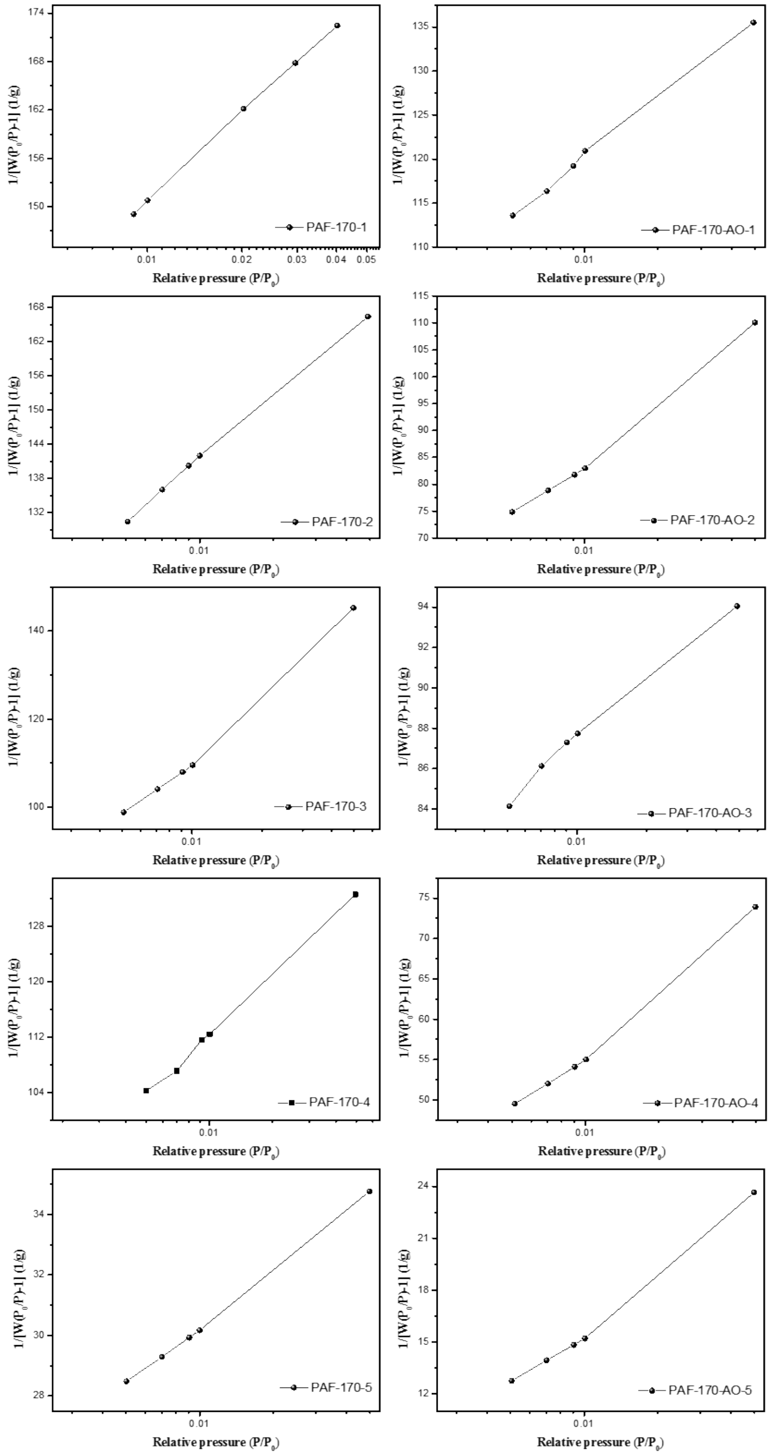

Figure S7 BET plots for PAF-170s and PAF-170-AOs.

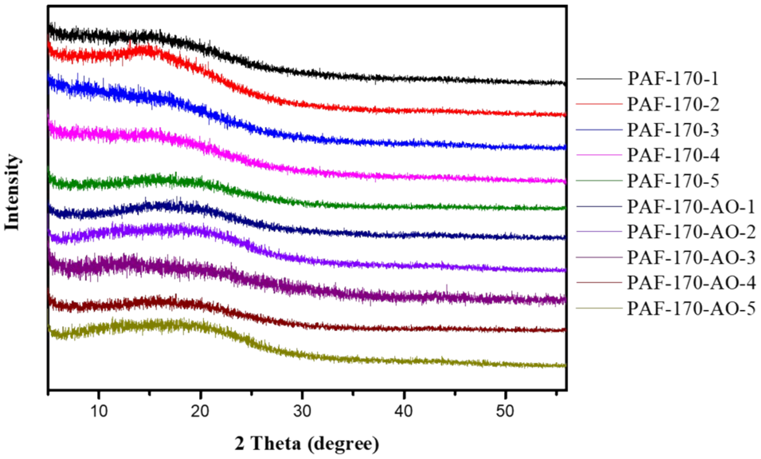

Figure S8 Powder X-Ray diffraction patterns of PAF-170s and PAF-170-AOs

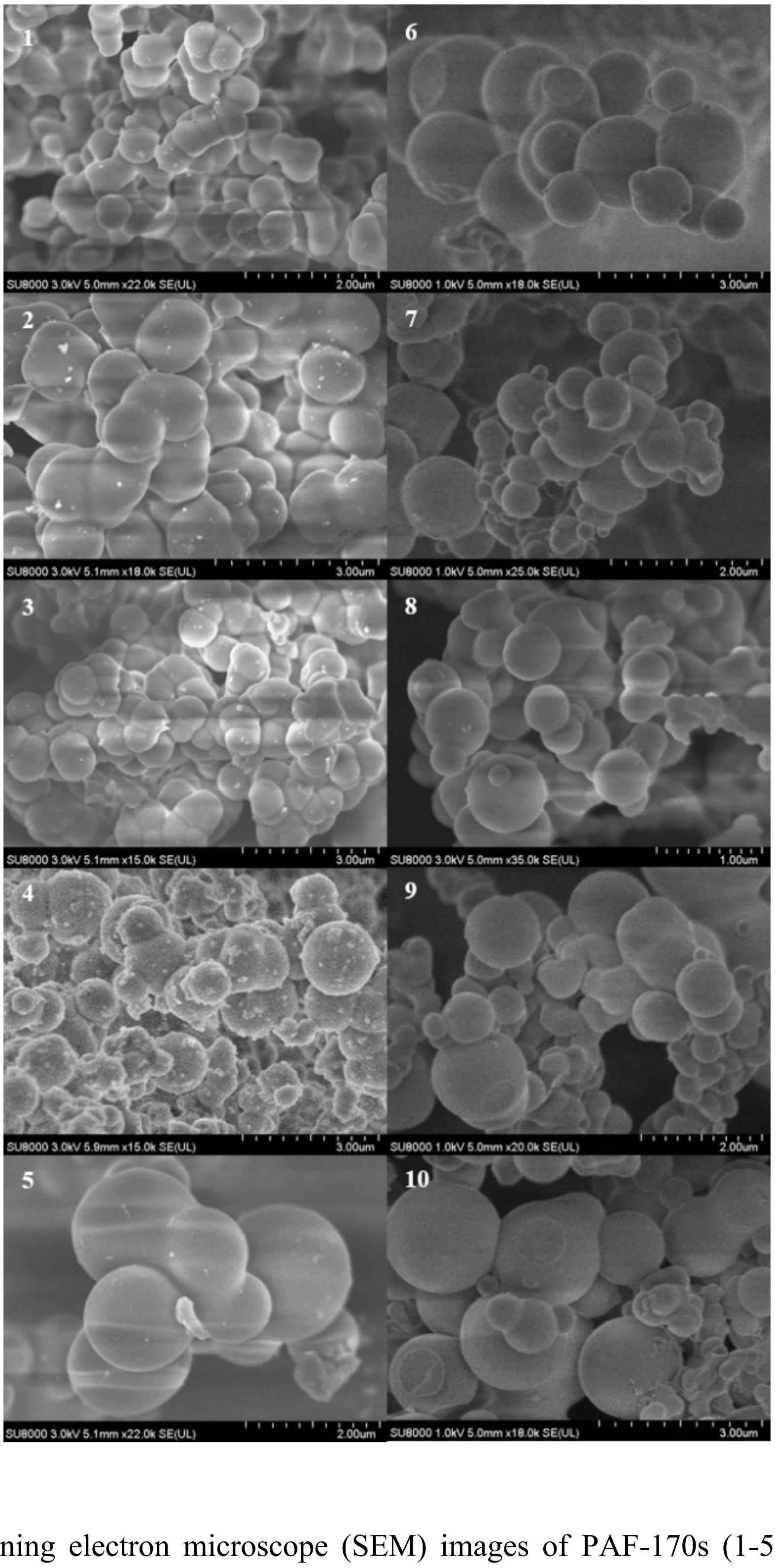

Figure S9 Scanning electron microscope (SEM) images of PAF-170s (1-5) and PAF-170-AOs (6-10).

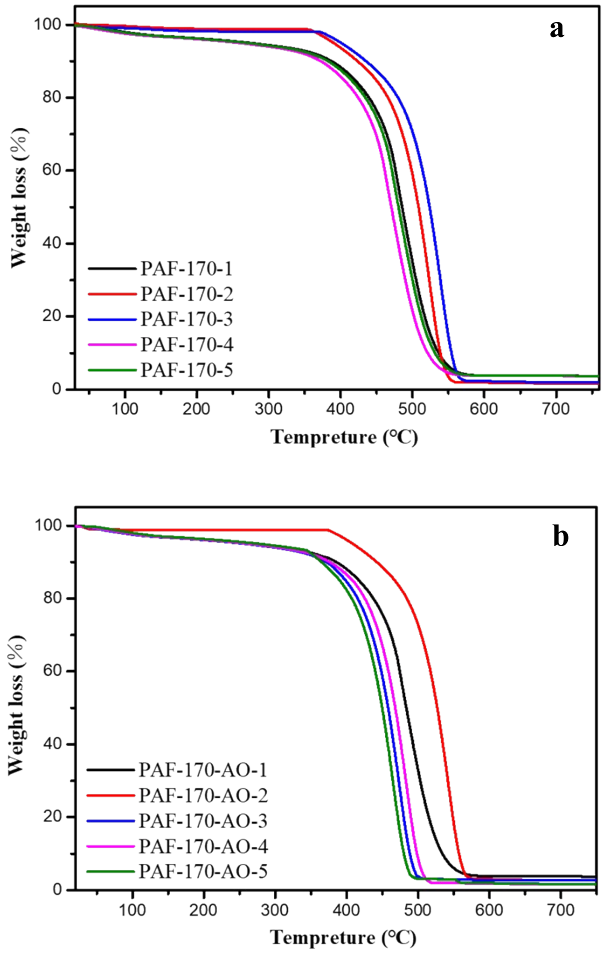

Figure S10 Thermogravimetric analysis (TGA) for (a) PAF-170s and (a) PAF-170-AOs, respectively.

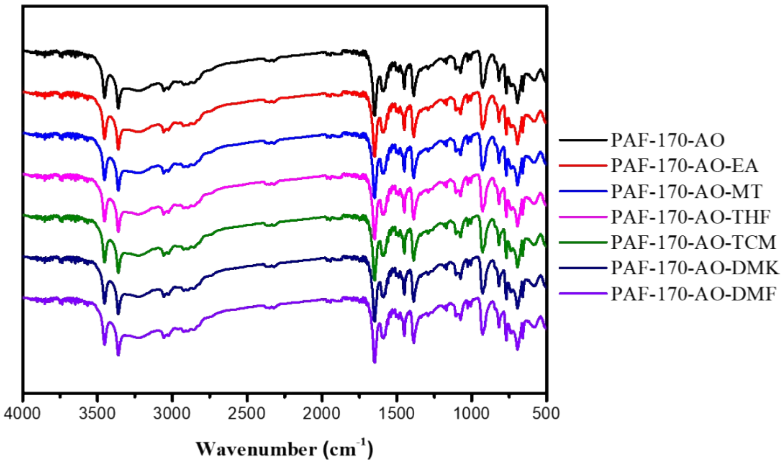

Figure S11 FT-IR spectra of PAF-170-AO before and after treatment with various solvents. Scanning range is 500-4000 cm^{-1}.

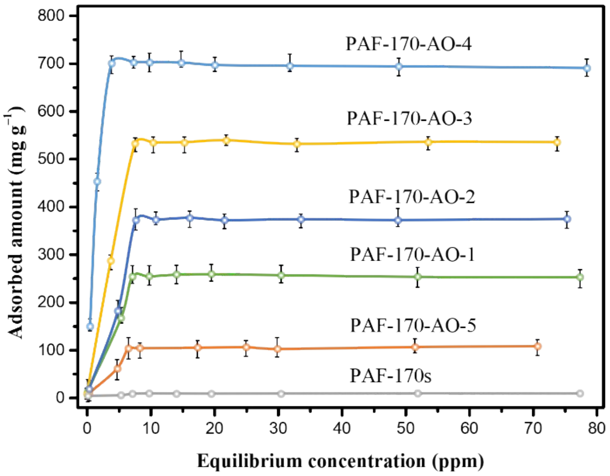

Figure S12 Uranium sorption isotherms for PAF adsorbents. PAF-170-AOs were suspended U(VI) solution from 1 to 85 ppm and stirred at a constant rate at room temperature.

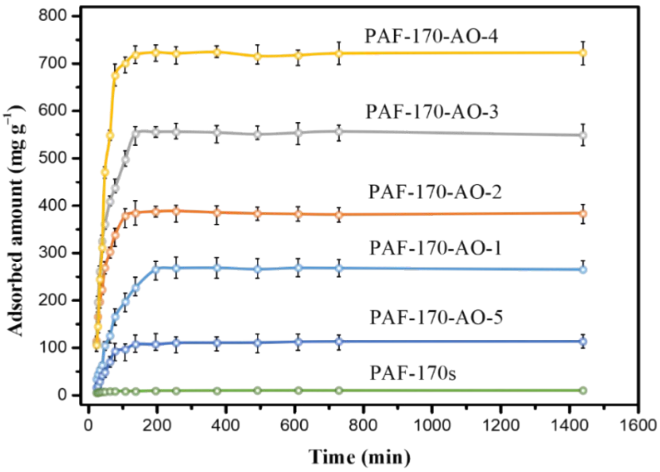

Figure S13 Uranium sorption kinetics for PAF adsorbents. PAF-170-AOs was suspended in 7 ppm U(VI) solution and stirred at a constant rate at room temperature.

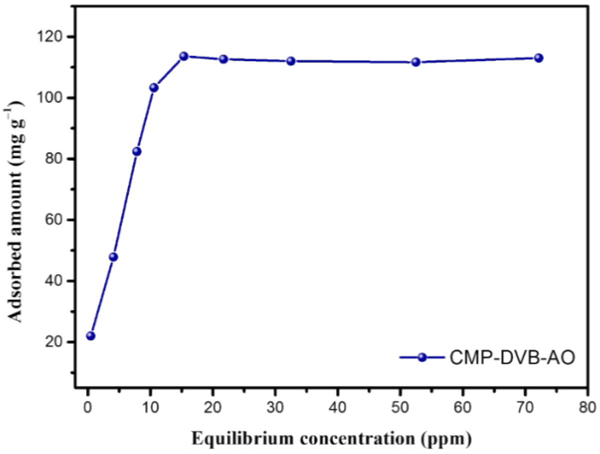

Figure S14 Uranium sorption isotherms for CMP-DVB-AO. CMP-DVB-AO was suspended in U(VI) solution from 1 to 75 ppm and stirred at a constant rate at room temperature.

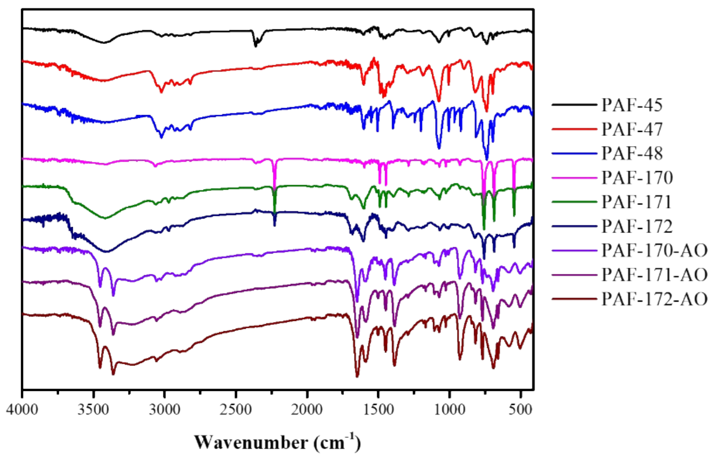

Figure S15 FT-IR spectra for PAF-45/46/48, PAF-170/171/172, and PAF-170/171/172-AO. Scanning range is 400-4000 cm^{-1}.

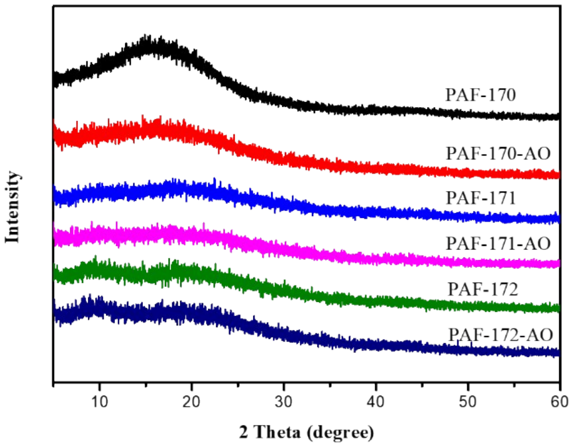

Figure S16 Powder X-Ray diffraction patterns of PAF-170/171/172 and PAF-170/171/172-AO.

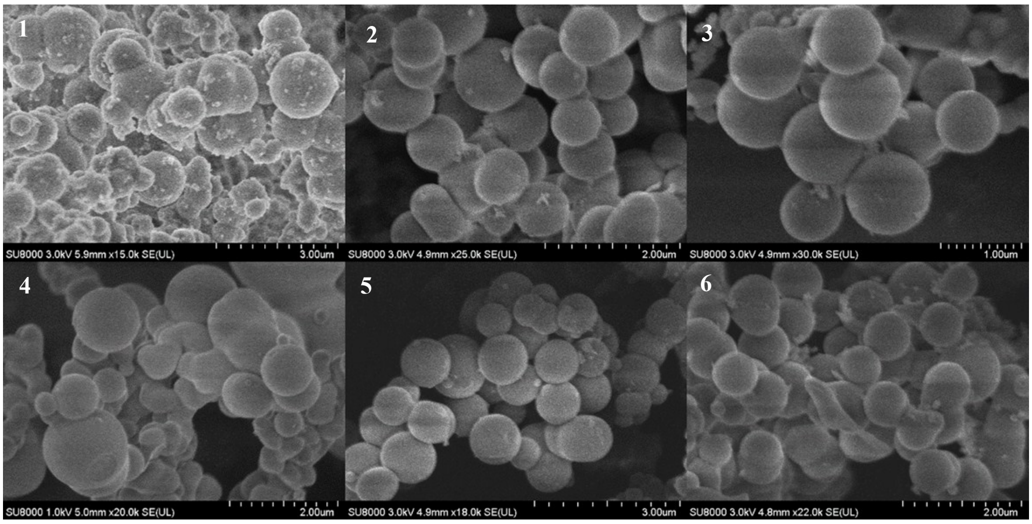

Figure S17 Scanning electron microscope (SEM) images of (1-3) PAF-170/171/172 and (4-6) PAF-170/171/172-AO.

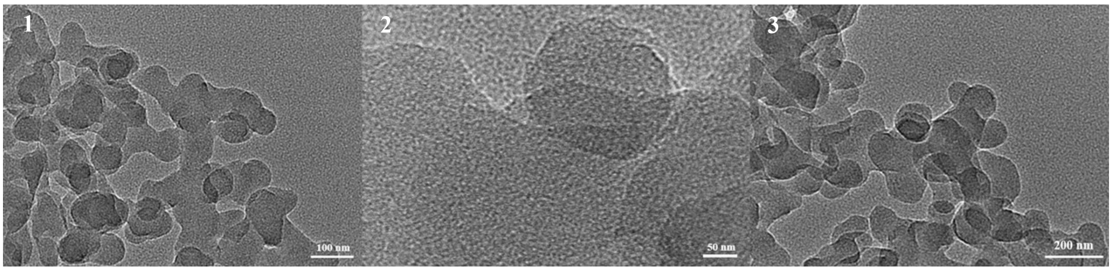

Figure S18 Transmission electron microscope (TEM) images of (1-3) PAF-170/171/172-AO.

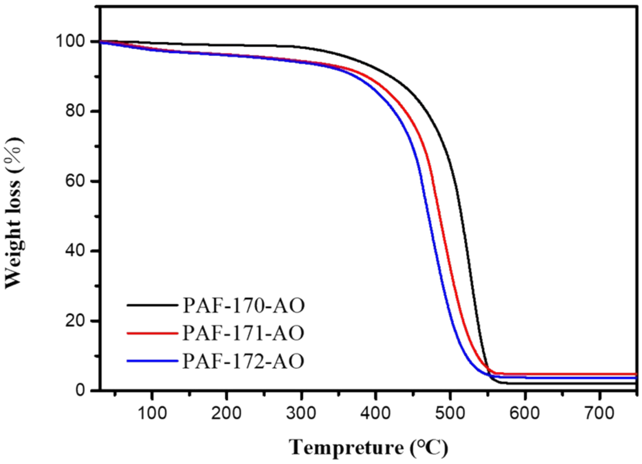

Figure S19 Thermogravimetric analysis (TGA) for PAF-170/171/172-AO.

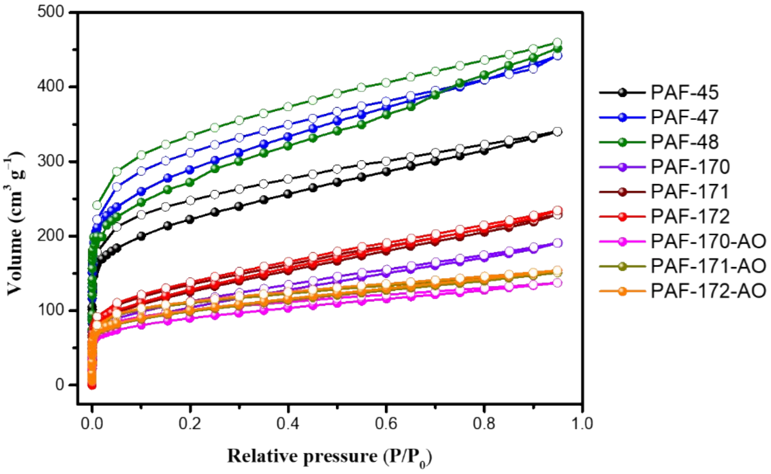

Figure S20 N_2 adsorption isotherms (solid icons) and N_2 desorption isotherms (hollow icons) collected at 77 K of PAF-45/47/48, PAF-170/171/172 and PAF-170/171/172-AO.

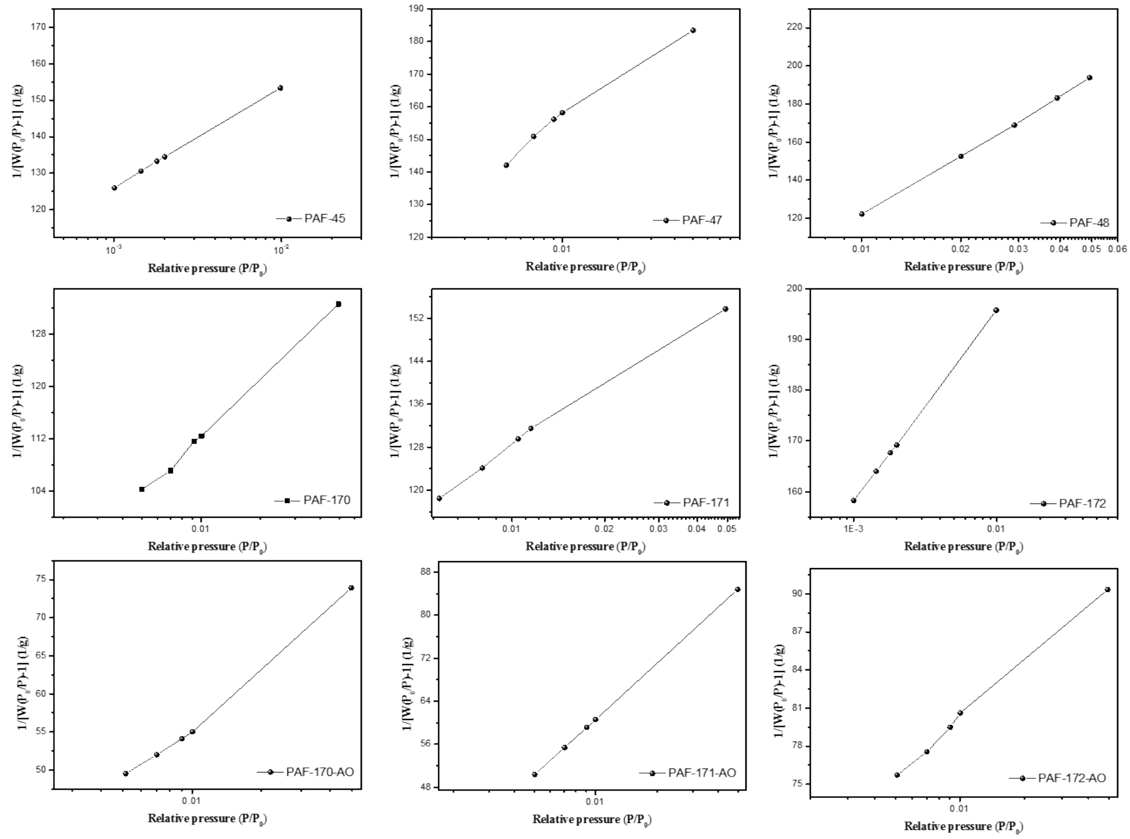

Figure S21 BET plots for PAF-45/47/48, PAF-170/171/172 and PAF-170/171/172-AO.

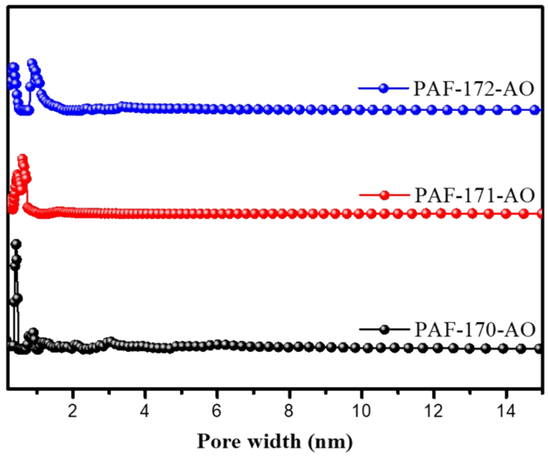

Figure S22 Pore size distribution collected at 77 K of PAF-170/171/172-AO.

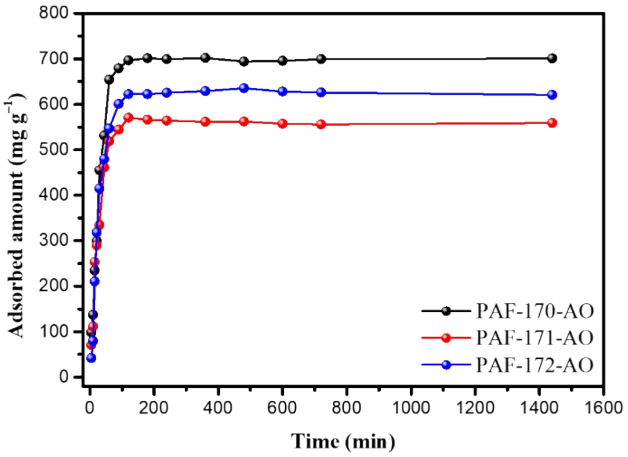

Figure S23 Uranium sorption kinetics for PAF-170/171/172-AO adsorbents. PAF-170/171/172-AO was suspended in 7 ppm U(VI) solution and stirred at a constant rate at room temperature.

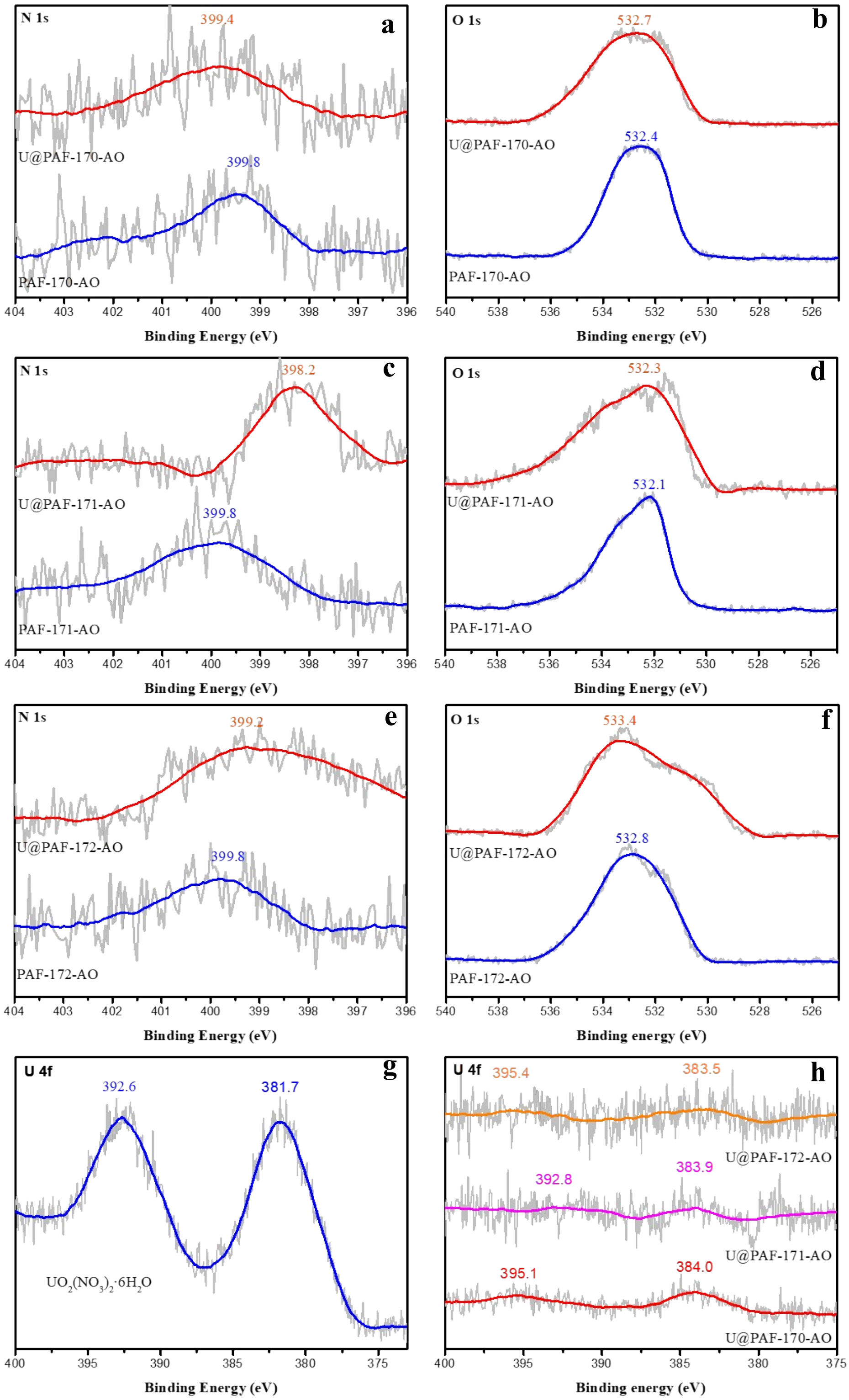

Figure S24 N *1s*, O *1s* and U *4f* XPS spectra of the uranium-adsorbed PAF-170-AO, PAF-171-AO and PAF-172-AO and $UO_2(NO_3)_2{\cdot}6H_2O$.

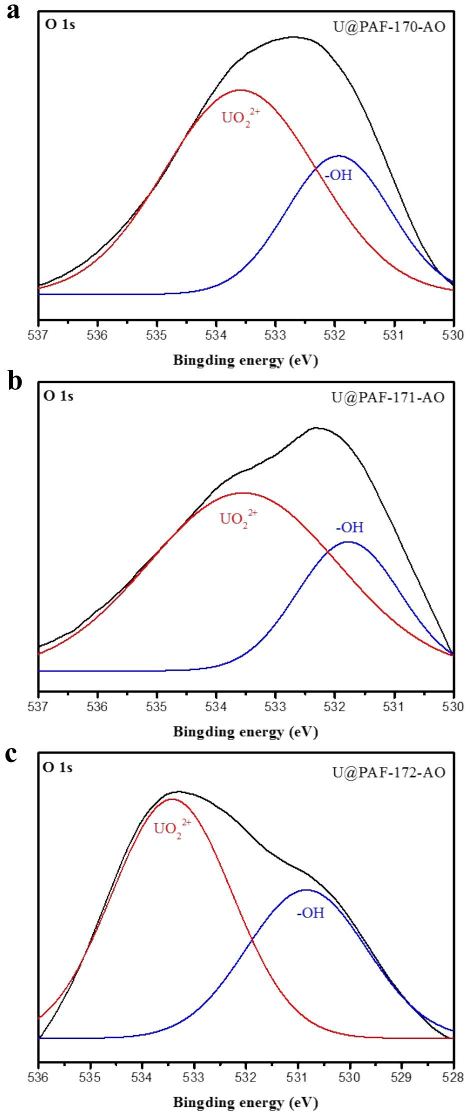

Figure S25 High resolution XPS spectra of O *1s* spectra of the uranium-adsorbed PAF-170-AO, PAF-171-AO, and PAF-172-AO. The O *1s* XPS peak (531.9 eV) of uranium-adsorbed PAFs can be divided into two signal peaks located at 532.4 and 533.4 eV. These two peaks are assigned to the O atoms in respective amidoxime and UO_2^{2+} groups of uranium-adsorbed PAFs

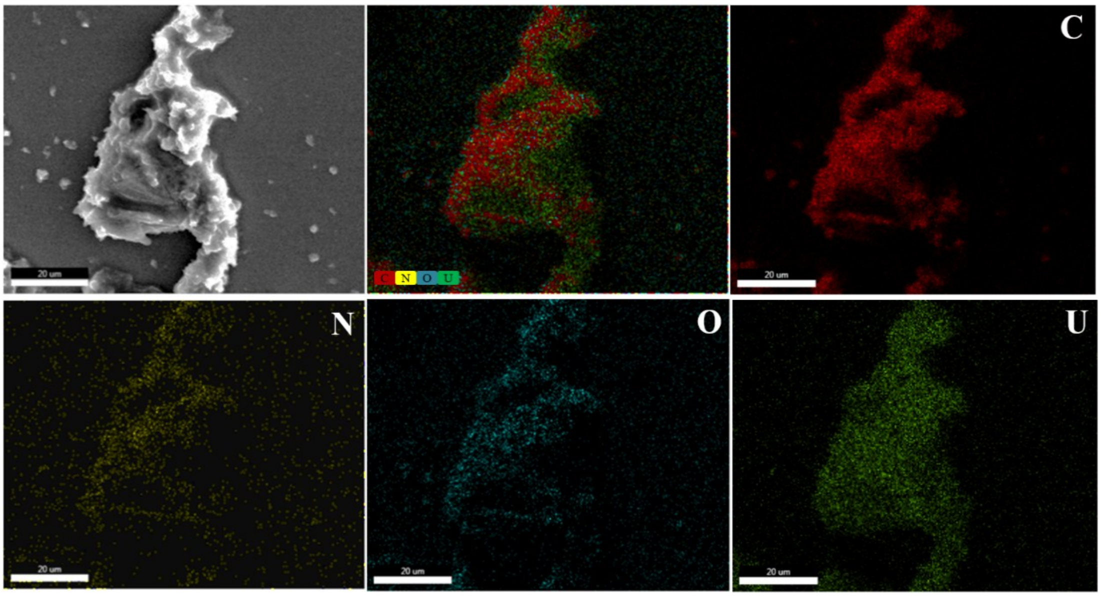

Figure S26 Corresponding EDX elemental mapping images of the elemental overlap of U@PAF-170-AO, C (red), N (yellow), O (blue), and U (green).

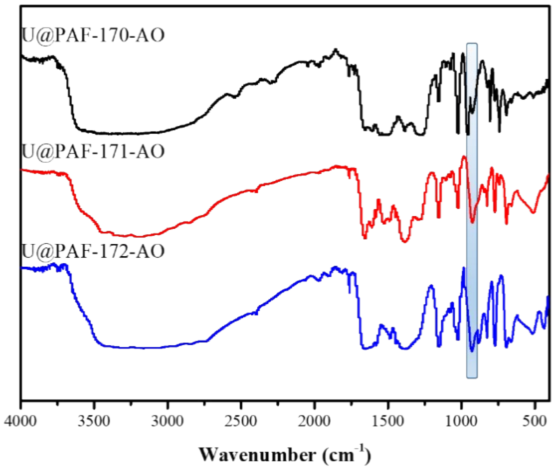

Figure S27 FTIR spectra of the uranium-contacted samples (U@PAF-170/171/172-AO). The UO_2^{2+} asymmetric normal vibration is around 900 cm^{-1}. Scanning range is 400-4000 cm^{-1}.

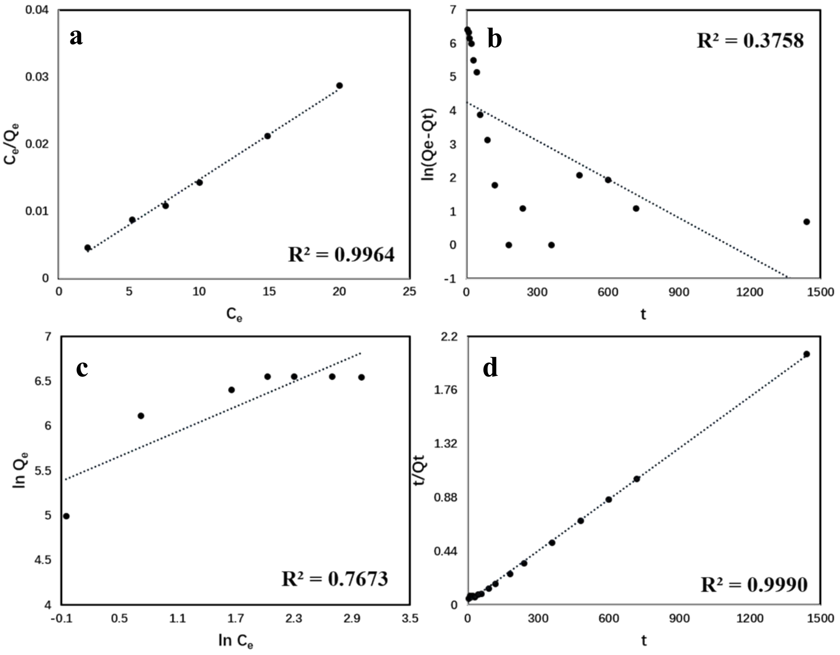

Figure S28 Uranium sorption isotherm (inset displays the linear regression by fitting the equilibrium data with the linear form of the (a) Langmuir adsorption model. (b) Pseudo-first-order kinetics. (c) Freundlich adsorption model. (d) Pseudo-second-order kinetics.

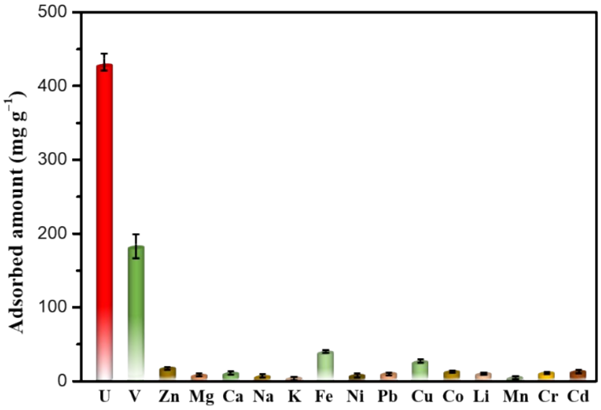

Figure S29 Uptake efficiency of PAF-170-AO-4 at 5 ppm various metal ions in 1 L simulated sea water. PAF-170-AO was suspended in 5 ppm various metal ions solution and stirred at a constant rate at room temperature.

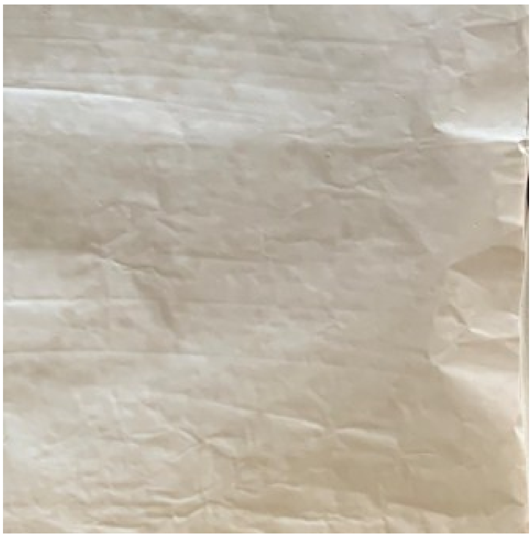

Figure S30 The composite fibre obtained by electrospinning the mixture of PAF material and polyacrylonitrile (PAN) in the 10% ratio of material.

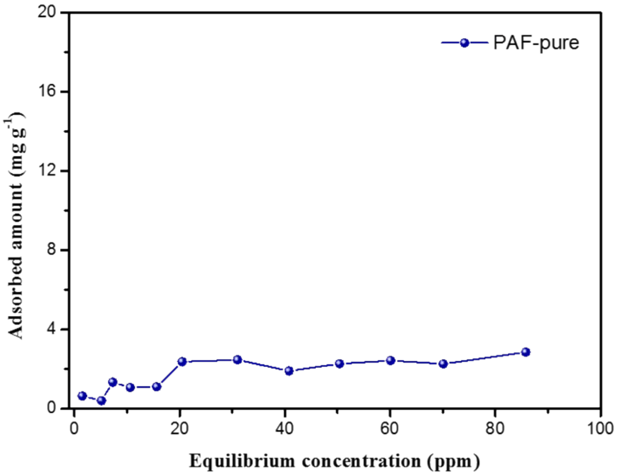

Figure S31 Uranium sorption isotherm for biphenyl-based pure PAF skeleton. PAF-pure were suspended in U(VI) solution with respective concentration ranged from 1 to 85 ppm and stirred for 24 h at room temperature. The pure PAF material has almost no adsorption capacity. This phenomenon proves the decisive role of amidoxime group for the extraction of uranium.

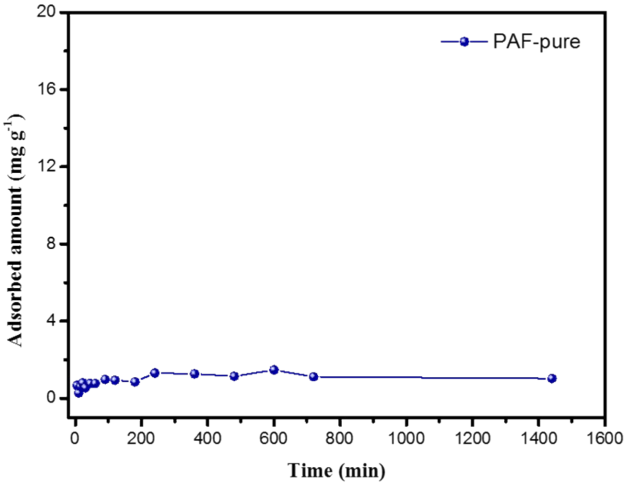

Figure S32 Uranium sorption kinetics for biphenyl-based pure PAF skeleton. PAF-pure was suspended in 7 ppm U(VI) solution and at room temperature.

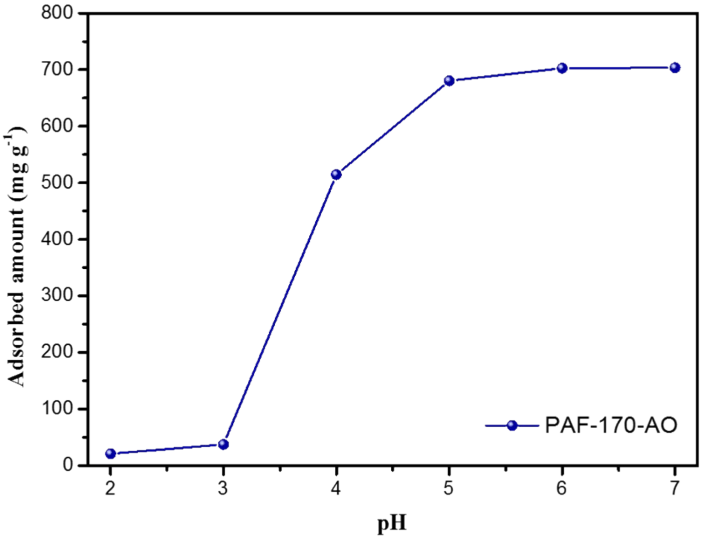

Figure S33 Uranium extraction performance of PAF-170-AO at different pH. PAF was suspended in 7 ppm U(VI) solution 24 h at room temperature.

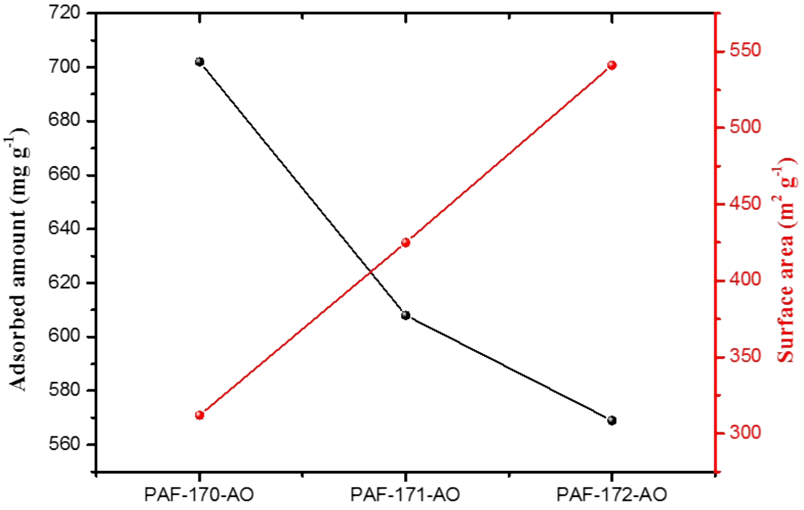

Figure S34 Relationship between extraction efficiency and adsorbed capatity of PAF adsorbents.

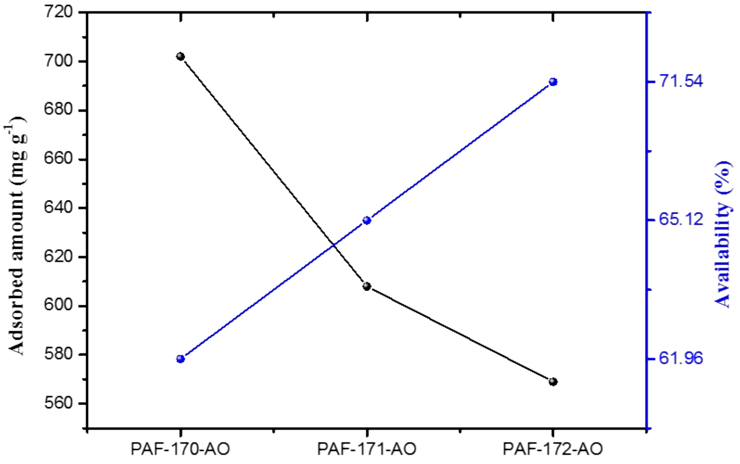

Figure S35 Relationship between extraction efficiency of uranium and available functional group of PAF adsorbents. The rigid monomers (*p*-terphenyl for PAF-171-AO and 1,3,5-triphenylbenzene for PAF-172-AO) with expanded structures compared with biphenyl (for PAF-170-AO) improve the porosity of adsorbents. The BET surface areas increase from 312 m^2 g^{-1} for PAF-170-AO to 425 and 541 m^2 g^{-1} for PAF-171-AO and PAF-172-AO, respectively. The expended porosity leads to the enhanced utilization ratio of amidoxime groups. However, the actual amount of amidoxime groups decreased from 4.68 (PAF-170-AO) to 3.92 (PAF-170-AO) and 3.34 (PAF-170-AO) mmol g^{-1}. The limited amount of amidoxime groups leads to the small adsorption capacity (702, 608, and 569 mg g^{-1} for PAF-170-AO, PAF-171-AO, and PAF-172-AO, respectively).

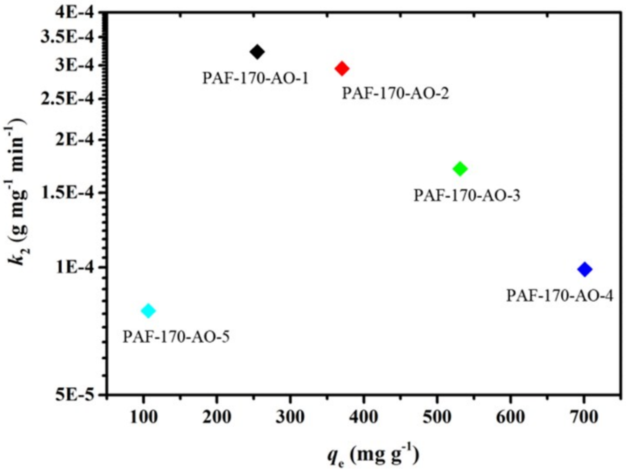

Figure S36 The *pseudo-second-order* adsorption constant k_2 (g·mg^{-1}·min^{-1}) for PAF-170-AOs.

Since the cyanophenyl unit may serve as the terminus of the skeleton, the expansion of porous network is limited with the increase of cyano group ratio. The most important feature is that the specific surface area decreases gradually from 478 (PAF-170-AO-1) to 126 m^2 g^{-1} (PAF-170-AO-5). As the cyano group doping ratios increased, the porosity of PAF materials decreases, which leads to the slow transport rate of uranyl ions in the particles. As observed, the k_2 value reduces gradually from 3.3*10^{-4} g mg^{-1} min^{-1} (PAF-170-AO-1) to 0.78*10^{-4} g mg^{-1} min^{-1} (PAF-170-AO-5).

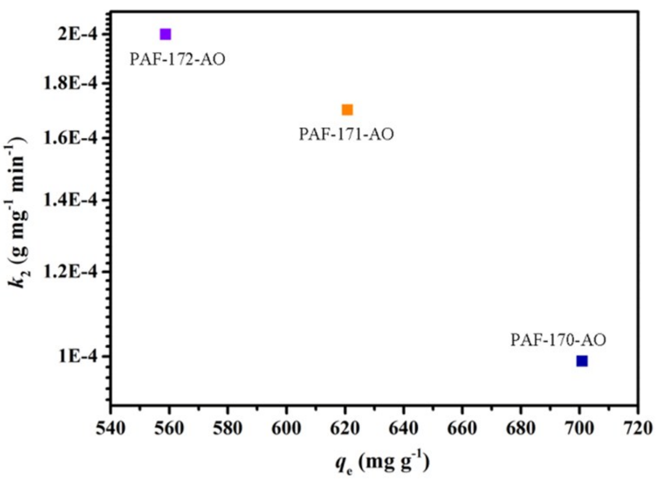

Figure S37 The *pseudo-second-order* adsorption constant k_2 (g·mg^{-1}·min^{-1}) for PAF-170/171/172-AO.

After optimizing the ratio of benzonitrile and phenyl building blocks (2:1), the respective rigid monomers (*p*-terphenyl and 1,3,5-triphenylbenzene) with expanded structures were utilized to improve the porosity of adsorbents. The expended porosity of porous materials leads to the rapid transport rate of uranyl ions in the particles. As observed, the k_2 value increases gradually from 0.95*10^{-4} g mg^{-1} min^{-1} (PAF-170-AO) to 2.0*10^{-4} g mg^{-1} min^{-1} (PAF-172-AO).

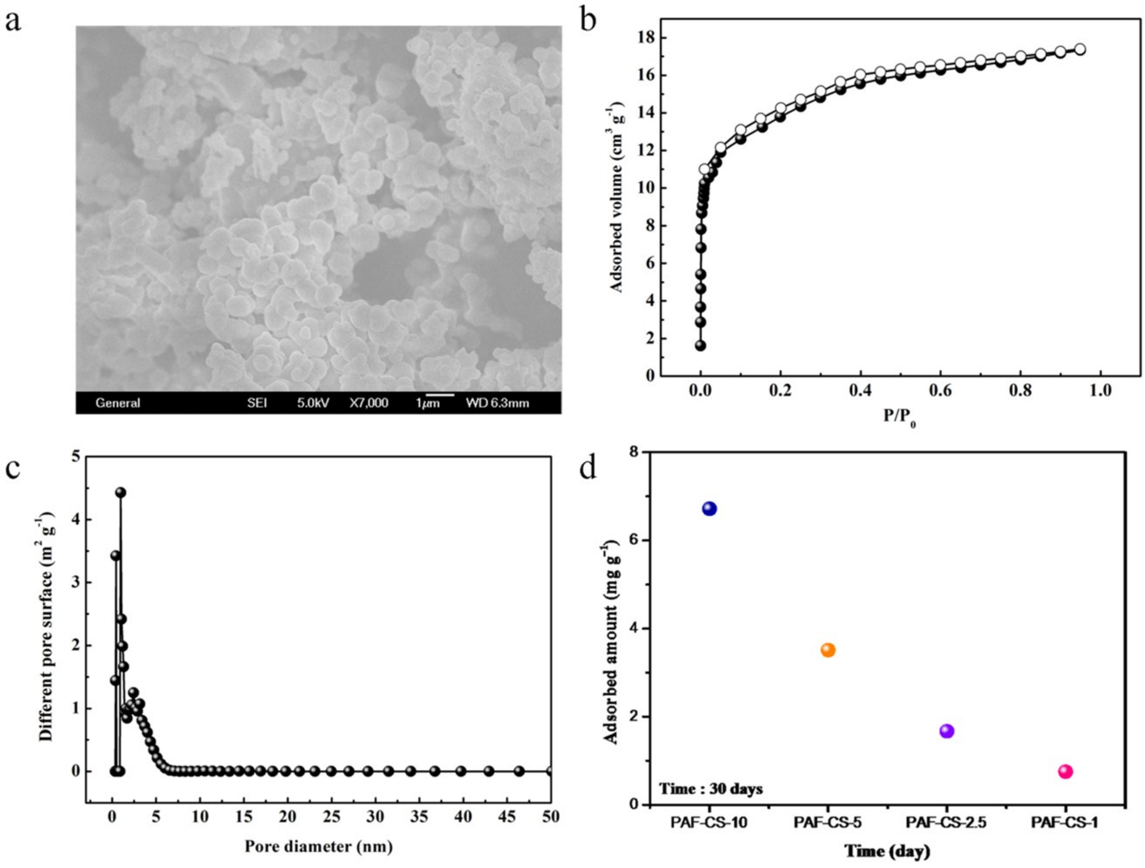

Figure S38 The detail characterization for PAF-loaded porous ceramic sheet (PAF-CS). (a) SEM image for PAF-CS with 10 wt% of PAF powder. (b) N_2 adsorption isotherms (solid icons) and N_2 desorption isotherms (hollow icons) collected at 77 K and (c) pore size distribution for PAF-CS with 10 wt% of PAF powder. (d) PAF-loaded porous ceramic sheets (PAF-CS) with the weight ratio in the range of 1, 2.5, 5, and 10% possess 0.047, 0.117, 0.234, and 0.468 mmol g^{-1} of amidoxime groups, respectively. Correspondingly, the uptake capacity for uranium in 30 days increases from 0.7 to 6.8 mg g^{-1}.

Table S1 Structural parameters for PAF-170/171/172-AO.

Sample	**Item**		
	Surface area (m^2 g^{-1})	**Pore volume (cm^3 g^{-1})**	**Pore size (nm)**
PAF-170	397	0.405	0.52
PAF-171	526	0.539	0.61
PAF-172	634	0.642	0.65
PAF-170-AO	312	0.311	0.45
PAF-171-AO	425	0.427	0.53
PAF-172-AO	541	0.524	0.60

Table S2 Elemental analysis for PAF-170/171/172-AO.

Sample	Element content (%)			
	C	H	O	N
PAF-170-AO	72.32	4.32	7.49	15.87
PAF-171-AO	74.48	6.40	6.27	12.85
PAF-172-AO	75.82	7.91	5.34	10.93

Contents of amidoxime groups in PAF samples.

Based on CHN elemental analysis, the oxygen contents for PAF-170/171/172-AO were 4.68 mmol·g^{-1}, 3.92 mmol·g^{-1} and 3.34 mmol·g^{-1}, respectively. Correspondingly, the actual amount of amidoxime groups of PAF-170/171/172-AO were also 4.68, 3.92, and 3.34 mmol g^{-1}, respectively. So the exact percentage of the amidoxime in PAF-170/171/172-AO were 27.61 %, 23.13 % and 19.71 %, respectively. The equilibrium adsorption capacity uptakes were 702, 608, and 569 mg g-1 for PAF-170-AO, PAF-171-AO, and PAF-172-AO, respectively, in ~7 ppm simulated seawater. As calculated by the ratio of the actual used amount and the theoretical amount, the usage ratios were determined to be 62.96% (PAF-170-AO), 65.12% (PAF-171-AO), and 71.54% (PAF-172-AO), Since Scholl reaction is a kind of electrophilic aromatic substitution reaction (EAS Reaction), the building monomer (cyanophenyl) with electron withdrawing cyano group inactivates its ortho and para positions. Especially, we adopted pure cyanophenyl to synthesize the PAF framework via Scholl reaction, and we couldn't get any solid product. Therefore, we believe the cyanophenyl unit serving as the terminus of the skeleton will restrict expansion of PAF network. As the amount of cyanophenyl increased, this compound inhibited the expansion of the porous network and resulted in fewer accessible adsorption groups within the internal space, resulting in the decrease of the utilization ratio of amidoxime groups.

Table S3 K_d values of PAF-170-AO for metal ions.

ion	U	V	Zn	Mg
K_d	9.37×10^6	6.29×10^5	12.07	44.99
ion	Ca	Na	K	Fe
K_d	20.20	4.45	8.44	49.18
ion	Ni	Pb	Cu	Co
K_d	40.82	262.44	188.18	70.39
ion	Li	Mn	Cr	Cd
K_d	28.40	159.83	689.57	487.56

Author Contributions

Z.L. carried out the experiments and performed the data interpretation. Z.L. and Y.Y. carried out the experiments and related characterizations. Z.L. and Y.Y. edited the manuscript. Y.Y. and G.Z. developed the concept, supervised the experiments and drafted the manuscript.